Article

Cell Reports

A BDNF-Mediated Push-Pull Plasticity Mechanism for Synaptic Clustering

Graphical Abstract

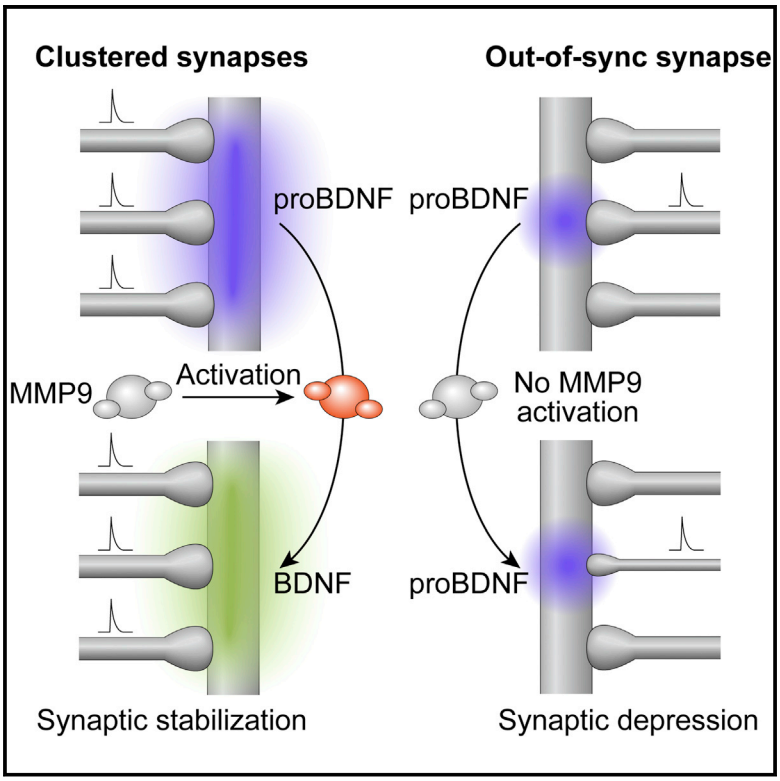

Authors

Dragos Niculescu,
Kristin Michaelsen-Preusse, Ülkü Güner,
René van Dorland, Corette J. Wierenga,
Christian Lohmann

Correspondence

c.lohmann@nin.knaw.nl

In Brief

Niculescu et al. found that synaptic clustering requires BDNF/TrkB signaling, activity of the proBDNF-to-BDNF conversion enzyme MMP9, and NMDA receptor activation. Their study delineates a push-pull plasticity mechanism where BDNF stabilizes clustered synapses while its precursor, proBDNF, depresses unclustered synapses, together ensuring robust clustering of synaptic inputs in developing neurons.

Highlights

- BDNF/TrkB signaling is required for functional synaptic clustering in hippocampus
- Exogenous BDNF activates "out of sync"; blocking TrkB eliminates "in-sync" synapses
- Clustering requires activity of MMP9, a proBDNF-to-BDNF conversion enzyme
- NMDAR activity downregulates locally desynchronized synapses upstream of proBDNF

Niculescu et al., 2018, Cell Reports *24*, 2063–2074
August 21, 2018
https://doi.org/10.1016/j.celrep.2018.07.073

CellPress

Cell Reports
Article

A BDNF-Mediated Push-Pull Plasticity Mechanism for Synaptic Clustering

Dragos Niculescu,[1,3] Kristin Michaelsen-Preusse,[1,5] Ülkü Güner,[1,6] René van Dorland,[4] Corette J. Wierenga,[4] and Christian Lohmann[1,2,7,*]
[1]Department of Synapse and Network Development, Netherlands Institute for Neuroscience, 1105 Amsterdam, the Netherlands
[2]Department of Functional Genomics, Center for Neurogenomics and Cognitive Research, VU University, Amsterdam, the Netherlands
[3]Department of Neurogenesis and Circuit Development, Vision Institute, 75012 Paris, France
[4]Department of Biology, Faculty of Science, Utrecht University, 3584 Utrecht, the Netherlands
[5]Present address: Division of Cellular Neurobiology, Zoological Institute, TU Braunschweig, 38106 Braunschweig, Germany
[6]Present address: Intralox LLC Europe, 1101 Amsterdam, the Netherlands
[7]Lead Contact
*Correspondence: c.lohmann@nin.knaw.nl
https://doi.org/10.1016/j.celrep.2018.07.073

SUMMARY

During development, activity-dependent synaptic plasticity refines neuronal networks with high precision. For example, spontaneous activity helps sorting synaptic inputs with similar activity patterns into clusters to enhance neuronal computations in the mature brain. Here, we show that TrkB activation and postsynaptic brain-derived neurotrophic factor (BDNF) are required for synaptic clustering in developing hippocampal neurons. Moreover, BDNF and TrkB modulate transmission at synapses depending on their clustering state, indicating that endogenous BDNF/TrkB signaling stabilizes locally synchronized synapses. Together with our previous data on proBDNF/p75^{NTR} signaling, these findings suggest a push-pull plasticity mechanism for synaptic clustering: BDNF stabilizes clustered synapses while proBDNF downregulates out-of-sync synapses. This idea is supported by our observation that synaptic clustering requires matrix-metalloproteinase-9 activity, a proBDNF-to-BDNF converting enzyme. Finally, NMDA receptor activation mediates out-of-sync depression upstream of proBDNF signaling. Together, these data delineate an efficient plasticity mechanism where proBDNF and mature BDNF establish synaptic clustering through antagonistic modulation of synaptic transmission.

INTRODUCTION

Neurons in the developing brain generate precisely connected networks already before the senses become active. Molecular guidance cues and trophic factors help neurons to grow axons and dendrites such that they can form specific connections with each other. Subsequently, spontaneous activity further refines synaptic connections to prepare the brain for computing sensory inputs and generating appropriate behavioral responses (Kirkby et al., 2013; Sanes and Yamagata, 2009).

At all stages of brain development, neurotrophins play a pivotal role for generating precisely connected networks. Neurotrophins regulate cell survival and cell death, and they determine synaptic fate by controlling synapse formation, potentiation, depression, and elimination (Park and Poo, 2013). In particular, brain-derived neurotrophic factor (BDNF) is present in the developing and adult forebrain and acts as a central organizer of synapse development and plasticity (Amaral and Pozzo-Miller, 2007; Edelmann et al., 2015; Harward et al., 2016; Vignoli et al., 2016). For example, BDNF regulates dendritic growth in an activity-dependent manner (Lai et al., 2012; McAllister et al., 1996); it promotes formation, unsilencing, and maturation of excitatory and inhibitory synapses (Cabezas and Buño, 2011; Huang et al., 1999; Mohajerani et al., 2007; Vicario-Abejón et al., 1998); and it contributes to the refinement of neuronal connections (Cabelli et al., 1995, 1997; Choo et al., 2017; review: Schinder and Poo, 2000).

Neurotrophins and their receptors are localized to synapses, and intrinsic neurotrophin signaling can be restricted to single synapses (review: Sasi et al., 2017). BDNF is present at presynaptic terminals (Andreska et al., 2014; Dieni et al., 2012) and postsynaptic specializations (Brigadski et al., 2005; Harward et al., 2016), and BDNF release occurs at synapses (reviewed in Lessmann and Brigadski, 2009). Correspondingly, the BDNF receptor tropomyosin-related kinase receptor B (TrkB) is enriched at pre- and postsynaptic structures (Drake et al., 1999; Wu et al., 1996). Moreover, endogenous BDNF can induce calcium transients at individual synapses (Lang et al., 2007), and glutamate uncaging triggers BDNF/TrkB signaling in individual spines (Harward et al., 2016; Tanaka et al., 2008). Together, these studies demonstrate that BDNF can refine networks with single-synapse precision.

The highest degree of precision of synaptic inputs on hippocampal and cortical neurons is represented by synaptic clustering: the co-arrangement of synapses with similar activity patterns and high synchronicity into short stretches of dendrites (Kleindienst et al., 2011; Takahashi et al., 2012). Synaptic clustering has been proposed to enhance neuronal computations and to increase the brain's sensitivity to sensory inputs in mature

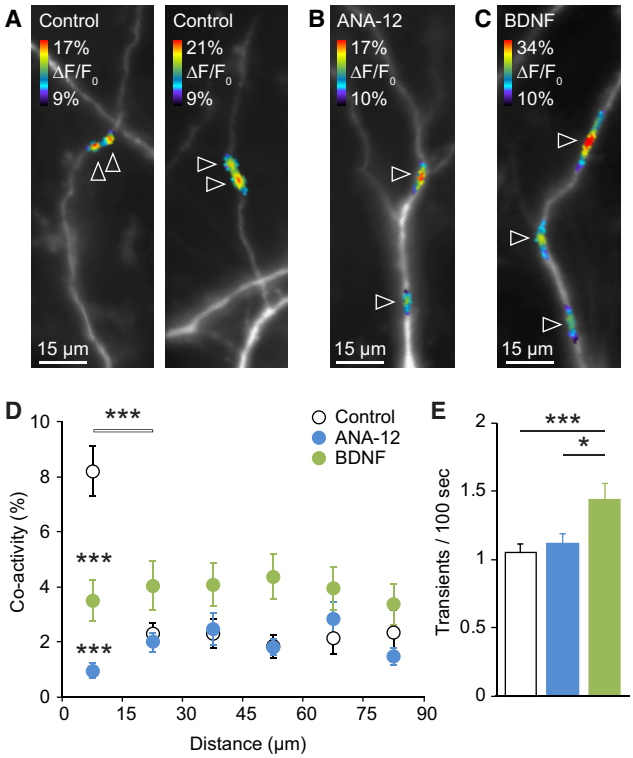

Figure 1. Altered TrkB Signaling Disrupts Synaptic Clustering

(A–C) Synaptic calcium transients in developing CA3 pyramidal cell dendrites.

(A) Control neurons showed synaptic clusters where calcium transients coincided at neighboring synapses.

(B) After incubation with the TrkB receptor antagonist ANA-12, synapses were desynchronized with their close neighbors during most of the events.

(C) Incubating slices with BDNF increased global co-activity, but local co-activity and synaptic clustering were perturbed.

(D) Co-activity levels of pairs of synapses with different inter-synaptic distances after a two-day incubation in the presence of ANA-12 or BDNF and for controls. Synaptic clustering was observed only in control conditions (n = 303 synapses from 16 cells; ***$p < 0.001$; unpaired two-tailed t test for the first two bins). After incubation with ANA-12 (n = 229 synapses from 7 cells) or BDNF (182 synapses from 6 cells), synaptic clustering was absent and co-activity levels for close neighbors were below control levels (ANA-12 versus control, BDNF versus control: ***$p < 0.001$; one-way-ANOVA and Fisher's post hoc test).

(E) Frequency of synaptic calcium transients at individual synapses. Synaptic activity was increased after BDNF incubation (***$p < 0.001$; *$p < 0.05$; one-way ANOVA and Fisher's post hoc test).

Error bars ± SEM. See also Figure S1.

animals (Iacaruso et al., 2017; Larkum and Nevian, 2008; Lavzin et al., 2012; Palmer et al., 2014; Poirazi and Mel, 2001; Smith et al., 2013). Synaptic clustering requires spontaneous neuronal activity to develop (Kleindienst et al., 2011). We previously showed that a local "out of sync-lose your link" plasticity mechanism, where locally desynchronized synapses become depressed, shapes synaptic clusters (Winnubst et al., 2015). This form of synaptic depression requires signaling of the BDNF precursor proBDNF at its receptor $p75^{NTR}$ (Winnubst et al., 2015). Because proBDNF and mature BDNF have antagonistic roles in cellular survival and synaptic function (Kaplan and Miller, 2000; Sasi et al., 2017), we tested here whether BDNF/TrkB signaling may be required for synaptic clustering as well, possibly interactively with proBDNF/$p75^{NTR}$ signaling.

Probing the effect of BDNF on single synapses, we provide evidence for a push-pull plasticity mechanism driven by spontaneous activity and NMDA receptor activation, where BDNF/TrkB signaling strengthens clustered synapses, proBDNF/$p75^{NTR}$ signaling depresses out-of-sync synapses, and MMP9-mediated proBDNF-to-BDNF conversion occurs at clustered synapses to efficiently sort synaptic inputs into correlated clusters along dendrites.

RESULTS

BDNF/TrkB Signaling Is Required for the Establishment of Synaptic Clusters

To investigate whether mature BDNF signaling is required for the establishment or maintenance of synaptic clustering, we first tested the effect of blocking its high-affinity receptor TrkB. Organotypic hippocampal slices, prepared from postnatal day (P) 3 mice, were incubated for 1 or 2 days and then exposed to the specific TrkB blocker ANA-12 (100 μM; Sigma-Aldrich) for 2 days. After a total of 3 or 4 days *in vitro* (DIV3–4) Cornu Ammonis 3 (CA3) neurons were loaded with the calcium indicator Oregon Green BAPTA-1 (OGB-1) using single-cell electroporation (Winnubst et al., 2015). Simultaneous patch-clamp and calcium-imaging experiments confirmed that local calcium transients represented excitatory synaptic inputs (Figure S1), as we have shown previously for developing rat hippocampal neurons (Kleindienst et al., 2011). When we recorded spontaneous synaptic calcium transients in CA3 pyramidal cell dendrites for 6 min in control slices, we found that neighboring synapses (<15 μm apart) were frequently co-active, and thus, synaptic inputs were clustered as described previously (Figures 1A and 1D; Kleindienst et al., 2011; Winnubst et al., 2015). In contrast, clustering was absent in neurons incubated with the TrkB blocker (Figures 1B and 1D). An additional control experiment demonstrated that DMSO (0.5%; Sigma-Aldrich; ANA-12 solvent) did not affect clustering (6.6% co-activity with synapses within 15 μm and 3.6% with synapses from 15 to 30 μm; n = 114 [15 μm], 116 [30 μm] synapses from 4 cells; $p < 0.05$; unpaired two-tailed t test). The complete absence of synaptic clustering after TrkB blockade indicated that endogenous BDNF-TrkB signaling is required for synaptic clustering.

Next, we asked whether application of exogenous BDNF might affect synaptic clustering as well. We found that also incubation with BDNF (200 ng/mL; Sigma-Aldrich) for 2 days abolished synaptic clustering (Figure 1C): there was no difference in co-activity levels between neighboring or distant synapses after BDNF incubation (Figure 1D). Overall synaptic activity was higher than after ANA-12 or control incubation (Figure 1E), possibly due to the facilitating effects of BDNF on synaptic function (reviewed in Park and Poo, 2013). Local co-activity levels were significantly reduced after ANA-12 or BDNF incubation compared to controls. Thus, both blockade and global activation of BDNF-TrkB signaling prevented synaptic clustering.

To identify the source of endogenous BDNF that is required for synaptic clustering, we downregulated BDNF expression

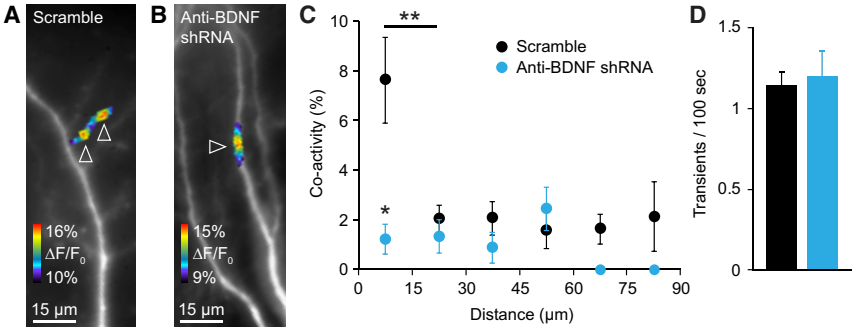

Figure 2. Downregulation of Postsynaptic proBDNF/BDNF Eliminates Synaptic Clustering

(A) Control neuron expressing a scrambled shRNA. Neighboring synapses were frequently co-active.

(B) Neuron expressing an anti-proBDNF/BDNF shRNA. Synapses were frequently desynchronized with their close neighbors.

(C) Synaptic clustering was absent after shRNA-mediated knockdown of BDNF (n = 61 synapses from 5 cells). Control cells transfected with scrambled shRNA showed robust clustering (n = 119 synapses from 5 cells; **p < 0.01; unpaired two-tailed t test for the first two bins). Co-activity levels for close neighbors were significantly lower after shRNA-mediated BDNF downregulation compared to control (*p < 0.05; unpaired two-tailed t test).

(D) The frequency of synaptic calcium transients at individual synapses was similar for scramble and shRNA.

Error bars ± SEM. See also Figure S2.

super-sparsely in individual CA3 neurons. We selected slices where 1–4 cells expressed either anti-BDNF or scrambled short hairpin RNA (shRNA). Anti-BDNF shRNA expression downregulated BDNF in HEK cells by >65% (Figure S2). Calcium imaging revealed that clustering was normal in neurons expressing scrambled shRNA; however, BDNF knockdown eliminated clustering entirely (Figures 2A–2C), demonstrating the importance of postsynaptic BDNF for synaptic clustering. Activity levels were not affected by BDNF knockdown (Figure 2D).

Together, these experiments showed that synaptic clustering required BDNF-TrkB signaling. Because global saturation of TrkB signaling abolished clustering, we hypothesized that endogenous BDNF was confined to clustered synapses to specifically stabilize clustered, but not locally desynchronized, synapses. In this scenario, globally applied BDNF would level out local differences in BDNF concentration, potentiate locally desynchronized synapses, and eventually abolish clustering.

BDNF Potentiates a Subpopulation of Synapses

To test whether exogenous BDNF indeed disrupts synaptic clustering by potentiating locally desynchronized synapses, we implemented an experiment that would allow us to monitor the effect of BDNF on individual synapses directly. BDNF (200 ng/mL in a 0.1% BSA solution) was applied focally with a glass electrode and placed approximately 10 μm away from a dendrite labeled with OGB-1, and 2 sets (3 min apart) of 3 pulses each (30 ms duration; 10 s apart) were delivered (Figure 3A) while monitoring injections in bright-field imaging (Figure 3B; Lang et al., 2007). We imaged dendrites for 6 min before BDNF application and 1 hr thereafter. We scored activity changes at functionally identified synapses after BDNF or control (0.1% BSA solution; Sigma-Aldrich) applications. We found that, 1 hr after BDNF (but not control) application, individual synapses exhibited large increases in the frequency of transmission events (Figure 3C). In addition, we observed synaptic activity at previously silent sites (Figure 3D). Plotting the change of synaptic activity in dependence of the distance of a given synapse from the pipette revealed that synapses within 60 μm radial distance from the pipette showed mean activity increases, but not beyond that distance (Figures 3E and 3F). Therefore, we restricted our further analysis to synapses within this range.

The total number of synaptic events per dendrite increased almost two-fold after BDNF application (Figure 3G). Synaptic activity decreased slightly after control puffs. Control experiments without local puffing demonstrated that there is no run down of synaptic activity and no change in clustering over a one-hour period in this slice preparation (Figure S3). Therefore, the physical impact of puffing may have affected synapse function slightly.

The BDNF-triggered increase in synaptic event frequency was the consequence of a mean increase in activity at previously active synapses and the emergence of transmission at previously inactive sites (Figures 3H and 3I). There was no significant change in amplitude for activated or not activated synapses after BDNF application (Figure 3J). The observation that BDNF triggered increases in frequency of synaptic transmission, but not amplitude, suggested that it increased presynaptic release probability rather than postsynaptic currents.

Responses of individual synapses differed and fell within one of four response categories: activated synapses showed transmission frequency increases of 1.5 transients/100 s and more (see Experimental Procedures for details). Unchanged synapses were active before and after BDNF application but did not increase in activity by 1.5 transients/100 s or more. New synapses were inactive during the baseline recordings but showed transmission after BDNF application, and eliminated synapses did not show any activity after BDNF application.

We found that the diversity of responses to BDNF application of individual synapses was not caused by initial differences in activity levels, because there was no significant difference in transmission rates before BDNF application between activated (1.22 ± 0.26/100 s; n = 16) and unchanged synapses (1.33 ± 0.13/100 s; n = 120; p = 0.51). Therefore, we asked whether response diversity might reflect the functional diversity of synapses of fundamentally different origins. In our slice cultures, CA3 pyramidal dendrites receive excitatory inputs mostly from mossy fibers and CA3 associative fibers. We performed experiments on synapses roughly 100 μm and more distally to the cell body, an area where associative fibers terminate. Because mossy, but not associative, fiber transmission onto CA3 pyramidal neurons can be blocked with the mGluR2/3

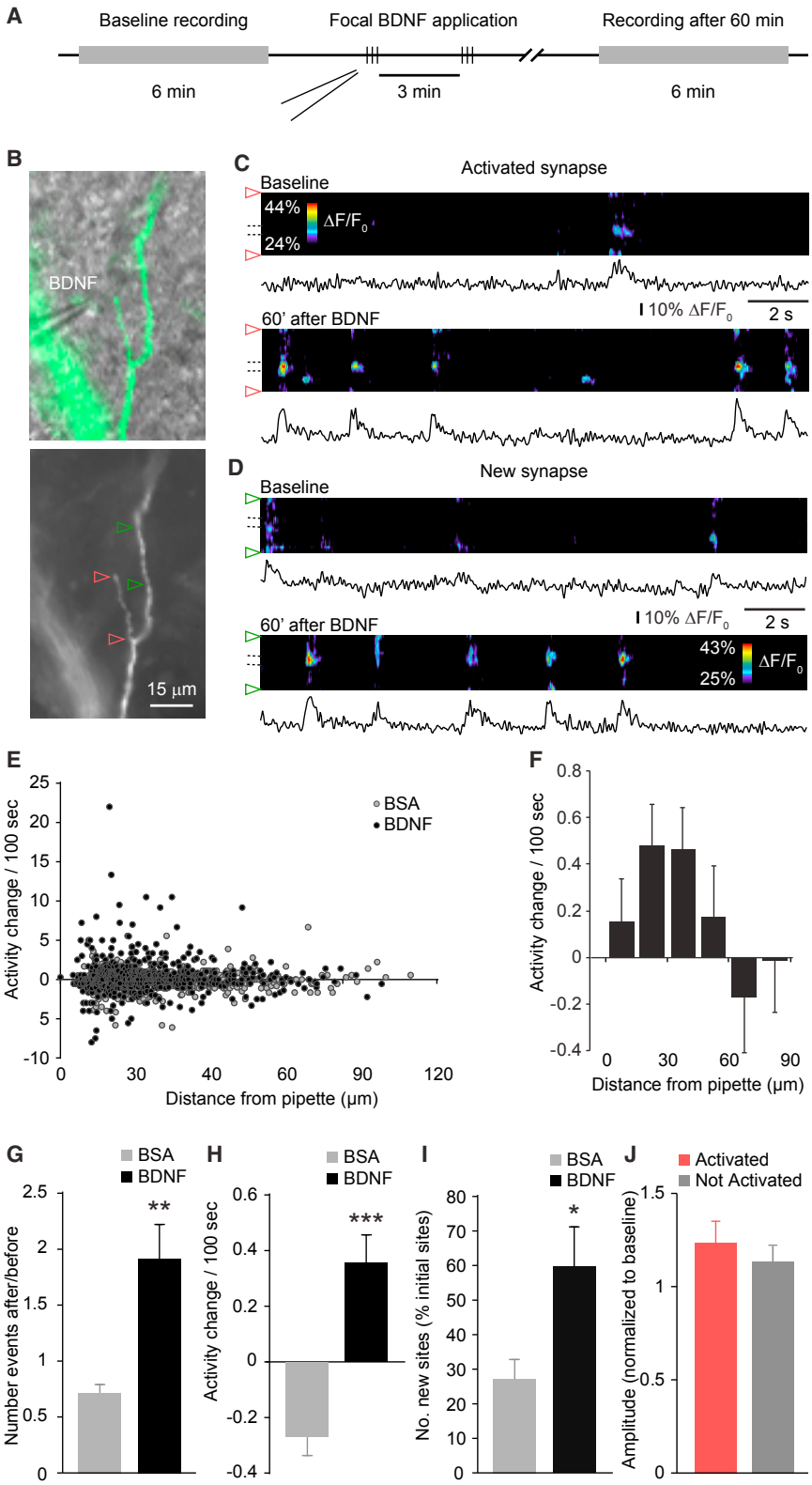

Figure 3. Focal BDNF Application Potentiates Synaptic Transmission

(A) Sequence of experimental procedure: baseline synaptic activity was recorded for 6 min. Subsequently, 3 BDNF pulses (30 ms each; 10 s interval) were applied twice to CA3 apical dendrites. Synaptic activity was recorded again after 60 min.

(B) CA3 pyramidal neuron loaded with OGB-1 by single-cell electroporation. A glass pipette containing BDNF was positioned in close proximity to two apical dendrites. Red and green arrowheads mark the stretches of dendrites that are shown in pseudo line scans in (C) and (D), respectively.

(C) Example of an activated synapse. Pseudo line scans of the dendrite marked by red arrowheads in (B) and $\Delta F/F_0$ traces of the synapse marked by dashed lines show a single spontaneous synaptic calcium transient before BDNF application (top). Synaptic transmission occurred repeatedly 1 hr after BDNF application (bottom).

(D) Example of a new synapse. This synapse was silent during baseline recordings but showed synaptic calcium transients after BDNF application.

(E) Individual synaptic activity changes plotted versus the distance from the delivery pipette (n = 407 synapses [BSA], 579 synapses [BDNF]).

(F) Averages of the binned individual changes shown in (E). The largest changes in synaptic activity occurred within 60 µm from the pipette.

(G) The total number of synaptic events per dendritic length increased almost two-fold 1 hr after BDNF application (n = 28 cells [BSA], 38 cells [BDNF]; $^{**}p < 0.01$; unpaired two-tailed t test).

(H) The frequency of transmission events at individual synapses increased compared to controls (n = 363 synapses [BSA], 537 [BDNF]; $^{***}p < 0.001$; unpaired two-tailed t test).

(I) Newly detected synapses as percentage of the total number of initial synaptic sites (n = 28 cells [BSA], 38 [BDNF]; $^{*}p < 0.05$; unpaired two-tailed t test).

(J) The amplitude of synaptic calcium transients did not differ between activated and not activated synapses.

Error bars ± SEM. See also Figures S3 and S4.

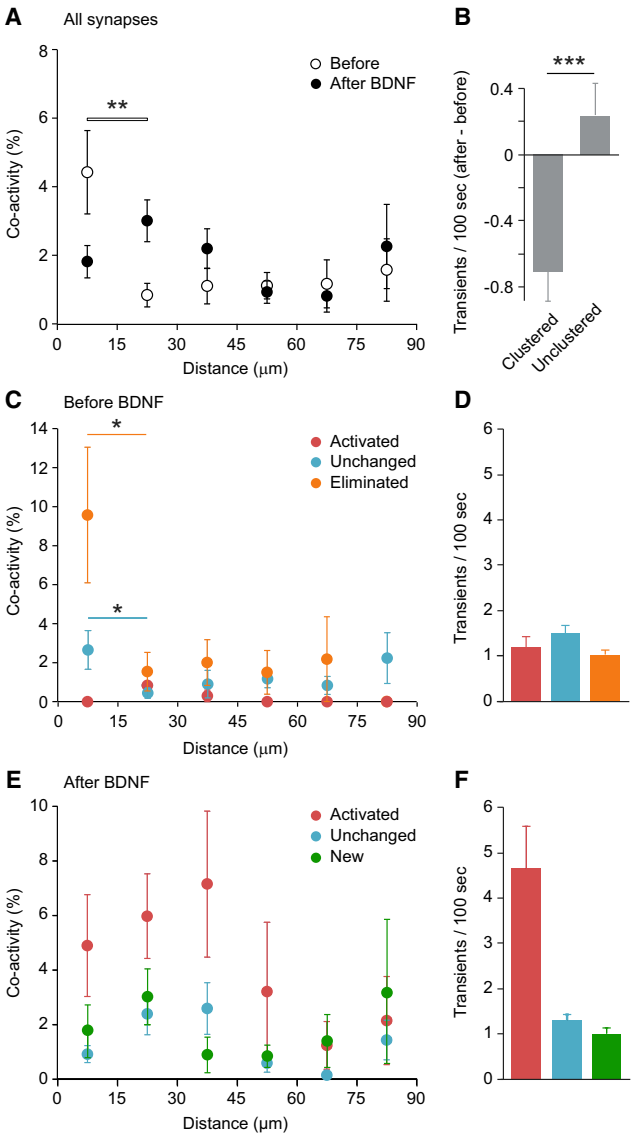

Figure 4. Focal BDNF Application Disrupts Synaptic Clustering through Clustering-State-Dependent Synaptic Modulation

(A) Co-activity levels of synapse pairs with different inter-synaptic distances, before and 1 hr after BDNF. Clustering of synapses can be found only before BDNF application (n = 121 synapses from 14 cells; **$p < 0.01$; unpaired two-tailed t test for the first two bins).

(B) BDNF-induced activity changes at individual synapses depended on their clustering state before BDNF application (n = 18 clustered synapses; n = 103 non-clustered synapses from 14 cells; ***$p < 0.001$; unpaired two-tailed t test).

(C) Co-activity levels for the three groups of synapses that were active during baseline recordings, categorized by their response 1 hr after BDNF. Synapses that were activated by BDNF were highly desynchronized before BDNF application. In contrast, unchanged and eliminated synapses showed different degrees of clustering (n = 14 synapses from 7 cells [activated], 71 synapses from 13 cells [unchanged], 36 synapses from 13 cells [eliminated]; *$p < 0.05$; unpaired two-tailed t test for the first two bins).

(D) Activity levels before BDNF application did not differ between these groups.

(E) Co-activity analysis for activated, unchanged, and newly formed synapses 1 hr after BDNF application. Neither group displayed clustering, although activated synapses showed higher global synchronicity than before BDNF application.

(F) Mean activity levels of activated synapses were 4 times higher than before BDNF application. New and unchanged synapses showed typical activity levels.

Error bars ± SEM. See also Figure S5.

agonist LY354740 (Kerr and Capogna, 2007; Richards et al., 2005), we used this drug to identify synaptic inputs. We found that calcium transients triggered by electric stimulation at synapses that were located 100 μm or more away from the soma were never silenced by LY354740 (1.5 μM; Ascent Scientific) bath application (Figures S4A and S4B). In contrast, transmission at more proximal synapses was entirely blocked by LY354740 (Figures S4C and S4D), suggesting that they represented mossy fiber inputs. Therefore, the synapses that we recorded at distal dendrites comprised a homogeneous population of CA3–CA3 associative inputs. This was further supported by our finding that responses to BDNF were distributed evenly across all synapses located between 100 and 300 μm distally from the cell body (Figures S4E and S4F). We concluded that the origin of synapses did not explain the differences between their responses to BDNF.

BDNF Potentiates Locally Desynchronized, but Not Clustered, Synapses

Next, we investigated how BDNF-triggered changes in activity of individual synapses related to synaptic clustering. When quantifying clustering before and one hour after focal BDNF application, we found that local co-activity was significantly reduced (Figure 4A; n = 121 synapses [before], 167 [after]; $p < 0.05$; unpaired two-tailed t test) in line with our observations after BDNF incubation (Figure 1). To address the question of how changes in activity at individual synapses may compromise synaptic clustering, we first asked whether BDNF affects clustered synapses differently from non-clustered ones. We split all synapses into clustered and unclustered synapses (see Experimental Procedures) and found that the activity change of unclustered synapses was much more positive than that of clustered synapses (Figure 4B). In fact, synapses that were activated by BDNF were not clustered at all and synapses whose activity levels did not change showed only moderate clustering before BDNF application, although eliminated synapses were highly clustered (Figure 4C). In addition, the local co-activity of eliminated synapses was significantly larger than that of unchanged or activated synapses (n = 36 eliminated, 71 unchanged, 14 activated synapses; $p < 0.05$; one-way-ANOVA and Fisher's post hoc test). The activity levels of activated, unchanged, or eliminated synapses were similar before BDNF application (Figure 4D). Thus, the differential response to BDNF reflected differences in clustering and not activity per se. Synapses were eliminated after particularly active out-of-sync neighbors had emerged and local co-activity had decreased (Figure S5), suggesting that competitive local interactions caused synapse elimination. Finally, we observed that activated, unchanged, and new synapses were mostly unclustered after BDNF application (Figure 4E). Activated synapses showed an increase in global co-activity levels, which

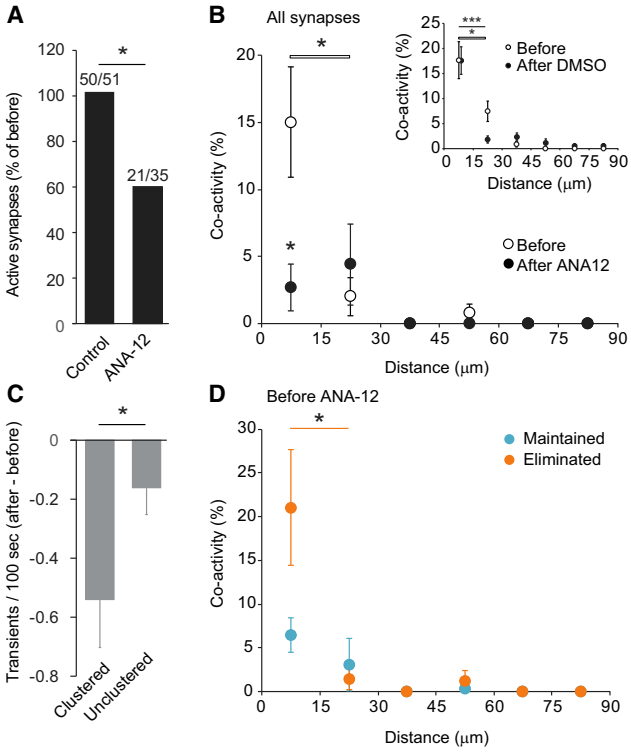

Figure 5. The TrkB Receptor Antagonist ANA-12 Disrupts Synaptic Clustering through Elimination of Locally Synchronized Synapses

(A) The number of active synapses was reduced after bath application of ANA-12 compared to control application of the solvent DMSO (0.7%; chi-square test; *p < 0.05).

(B) Co-activity levels of synapse pairs with different inter-synaptic distances, before and 10 min after ANA-12. Synapses were clustered before, but not after, ANA-12 application (n = 34 synapses from 3 cells; *p < 0.05; unpaired two-tailed t test for the first two bins). Local co-activity was significantly reduced after ANA-12 application (n = 34 synapses [before], 20 [after]; *p < 0.05; unpaired two-tailed t test). Inset: bath application of the solvent DMSO did not affect clustering (n = 46 before, 50 synapses after DMSO; *p < 0.05; ***p < 0.001; unpaired two-tailed t tests for the first two bins).

(C) ANA-12-induced activity changes at individual synapses depended on their clustering state before ANA-12 application (n = 21 clustered synapses; n = 13 non-clustered synapses from 3 cells; *p < 0.05; unpaired two-tailed t test).

(D) Co-activity levels of synapses before ANA-12 application. Synapses that were eliminated after ANA-12 application showed significant clustering before ANA-12 application, in contrast to maintained synapses (n = 20 synapses from 3 cells [eliminated], 14 synapses from 3 cells [maintained]; *p < 0.05; unpaired two-tailed t test for the first two bins).

Error bars ± SEM.

contributed to the elimination of clustering. Transmission frequency at activated synapses was 4 times higher after BDNF application and new synapses reached roughly average activity levels (Figure 4F). Together, these experiments confirmed the prediction that exogenous BDNF specifically potentiated unsynchronized synapses and activated silent synapses. In contrast, BDNF application did not potentiate clustered synapses, perhaps because endogenous BDNF was present and effective at clusters and thus prevented an additional effect of exogenous BDNF at clustered synapses.

TrkB Blockade Eliminates Clustered, but Not Locally Desynchronized, Synapses

The previous observations indicated that endogenous BDNF stabilized clustered synapses. To test whether the BDNF receptor TrkB is required for maintaining clustered synapses as well, we investigated the short-term effect of its blocker ANA-12 on individual synapses. We found that 10-min bath applications of ANA-12 reduced the number of active synapses significantly, compared to control solution (0.7% DMSO; Figure 5A). In addition, ANA-12 application, but not control solution, perturbed synaptic clustering (Figure 5B) and significantly reduced local co-activity (n = 34 synapses [before], 20 [after]; $p < 0.05$; unpaired two-tailed t test). Analysis of the relationship between the clustering state of individual synapses and their sensitivity to ANA-12 revealed that clustered rather than unclustered synapses were depressed or eliminated after TrkB blockade (Figures 5C and 5D).

ProBDNF-to-BDNF Conversion Enzyme MMP9 Is Required for Synaptic Clustering

BDNF is synthesized as proBDNF and then converted to mature BDNF. Previously, we found that proBDNF-p75^{NTR} signaling mediates out-of-sync local depression (Winnubst et al., 2015). Because we observed here that BDNF-TrkB signaling is required for synaptic clustering, most likely through stabilizing locally synchronized synapses, we reasoned that proBDNF-to-BDNF conversion might be an important switch for generating synaptic clustering. A prime candidate among the known conversion enzymes was matrix metalloproteinase 9 (MMP9), a member of a major family of extracellular proteinases. MMP9 is highly expressed in the hippocampus at the here investigated ages (Aujla and Huntley, 2014; Murase and McKay, 2012) and has been shown to convert proBDNF to BDNF in an activity-dependent manner (Dziembowska and Wlodarczyk, 2012; Ethell and Ethell, 2007). Therefore, we tested the effect of MMP9 Inhibitor I (50 nM; Calbiochem) on synaptic clustering. Dendrites were imaged for 6 min to evaluate initial co-activity levels and then MMP9 Inhibitor I was applied to the recording chamber for 10 min. Subsequently, we recorded synaptic calcium transients again for 6 min. Our results showed a complete disruption of clustering 10 min after exposure to MMP9 Inhibitor I (Figure 6A) and a significant decrease in local co-activity levels (n = 167 synapses [before], 174 [after]; $p < 0.001$; unpaired two-tailed t test), although overall activity levels were slightly increased (Figure 6B). In control recordings, we imaged calcium transients before and 10 min after bath application of MMP2 Inhibitor III (120 nM; Calbiochem). MMP2 is the only other member of the gelatinase subgroup of metalloproteinases, and its developmental expression pattern and enzymatic characteristics are very similar to those of MMP9 (Aujla and Huntley, 2014; Murase and McKay, 2012), except that MMP2 does not convert proBDNF to mature BDNF (Je et al., 2012). Blocking MMP2 activity had no effect on local co-activity (n = 79 synapses [before], 81 [after]; $p > 0.05$; unpaired two-tailed t test) or absolute activity levels of individual synapses (Figures 6C and 6D). Blocking tissue plasminogen activator (tPA), another proBDNF-mature BDNF conversion enzyme, did not block synaptic clustering either (Figure S6). Together, our results indicate that specifically MMP9-dependent proBDNF-to-BDNF conversion is crucial to synaptic clustering.

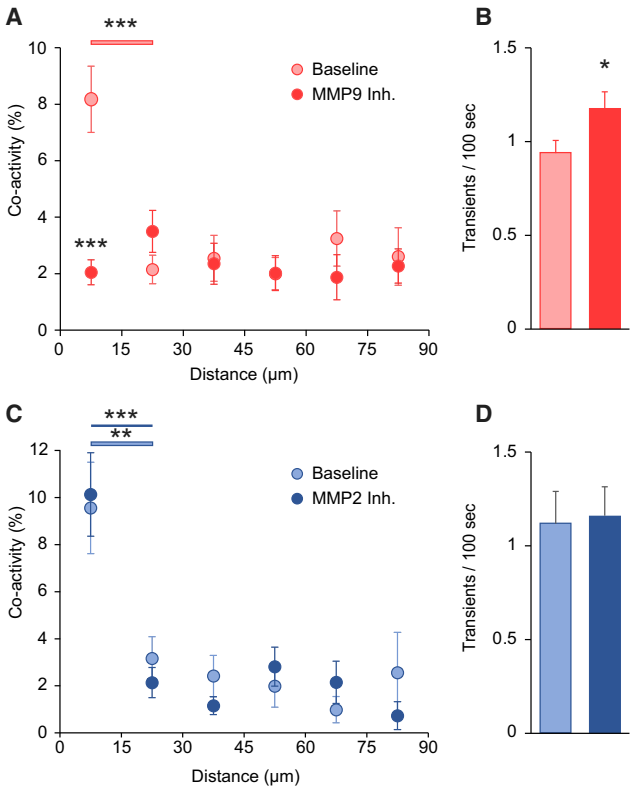

Figure 6. Matrix Metalloproteinase 9 Is Required for the Maintenance of Synaptic Clustering

(A) Co-activity levels of synapse pairs with different inter-synaptic distances, before and 10 min after application of MMP9 inhibitor I (50 nM). Synapses showed robust clustering during baseline recordings (n = 167 synapses from 5 cells; ***p < 0.001; unpaired two-tailed t test for the first two bins). In contrast, 10 min exposure to MMP9 Inhibitor I entirely abolished clustering. Co-activity values for the first bin were significantly lower than during baseline recordings (n = 174; ***p < 0.001; unpaired two-tailed t test).

(B) Activity was increased slightly after MMP9 application (*p < 0.05; unpaired two-tailed t test).

(C) Control experiment with MMP2 Inhibitor III (120 nM), showing no difference in co-activity levels between the 15-μm bins of baseline and 10 min after inhibitor application. In both conditions, synaptic clustering was present (n = 79 synapses from 4 cells for before [**p < 0.01, unpaired two-tailed t test for the first two bins], and 81 synapses for after [***p < 0.001, unpaired two-tailed t test for the first two bins] the inhibitor).

(D) Synaptic activity did not change after application of MMP2 Inhibitor III. Error bars ± SEM. See also Figure S6.

NMDA Receptor Activation Is Required for Out-of-Sync Depression

Both proBDNF and mature BDNF release are dependent on neuronal activity and NMDA receptor activation (Hartmann et al., 2001; Harward et al., 2016; Nagappan et al., 2009; Orefice et al., 2016). In addition, we previously demonstrated that synaptic clustering is activity- and NMDA-receptor-dependent (Kleindienst et al., 2011). Therefore, we tested the role of NMDA receptor activation in out-of-sync depression, a proBDNF-mediated plasticity mechanism that can generate synaptic clustering (Winnubst et al., 2015). Single synapses were activated (0.1 Hz) using a glass electrode, placed in the stratum radiatum of the CA3 region, and baseline transmission success rates of individual synapses were measured using calcium imaging during two 2-min recordings (Figure 7A). The NMDA receptor antagonist AP5 (50 μM; Tocris) was washed into the recording chamber during an additional 2-min recording. Subsequently, we applied 0.1 Hz stimulation for 12 min—a stimulus known to induce depression of synaptic transmission success rates (Winnubst et al., 2015)—in the presence of AP5. During the presence of AP5, postsynaptic calcium transients were reduced to <30% of stimulations on average (Figure 7A). Postsynaptic responses were blocked entirely in some synapses or showed strongly reduced amplitudes in the remaining ones (32.5% ± 11.8% of control levels; not shown). Washout of AP5 was monitored during two subsequent 2-min recordings, and the final success rates were evaluated during two following recordings (at least 12 min after begin of washout). At control synapses, success rates were significantly depressed after out-of-sync stimulation (Figures 7B and 7C). In contrast, synapses that received the depression stimulus in the presence of AP5 remained unaffected: there was no significant difference between success rates before and after stimulation (Figures 7B and 7C). Whereas NMDA receptor blockade prevented synaptic depression after out-of-sync stimulation, it did not prevent synaptic depression upon application of uncleavable proBDNF (Figures 7B and 7C).

Together, these experiments indicated that NMDA receptor activation upstream of proBDNF was required for out-of-sync synaptic depression. Because low-frequency stimulation as used here (0.1 Hz) activates postsynaptic, but not presynaptic, NMDA receptors in the hippocampus (McGuinness et al., 2010) and NMDA receptor activation can trigger proBDNF release (Nagappan et al., 2009), this result suggested that NMDA-receptor-dependent postsynaptic proBDNF release caused synaptic depression at out-of-sync synapses (Figures 7D and 7E).

DISCUSSION

BDNF is a powerful modulator of synaptic function, and it is essential for wiring central neuronal networks. Here, using an imaging approach to follow changes in activity at individual synapses in intact tissue, we identified BDNF-TrkB signaling as a requirement for synaptic clustering and delineated a proBDNF/BDNF push-pull plasticity mechanism for synaptic clustering in developing neurons.

Previous studies showed that BDNF potently activates developing networks and synapses (Berninger and Poo, 1996). Surprisingly, we find that BDNF potentiates synapses differentially. However, neither synapse type, activity level, nor position along the dendrite correlates with BDNF-induced synaptic potentiation. Instead, exogenous BDNF potentiates synapses that are out of sync with their neighbors, but not clustered synapses. The most parsimonious explanation for this finding is that endogenous BDNF is present and active at clustered synapses and thus prevents any additional effect of exogenously applied BDNF. Conversely, the absence of endogenous BDNF at out-of-sync synapses renders them sensitive to potentiation through exogenous BDNF. Together with our finding that signaling of the high-affinity BDNF receptor TrkB is required for synaptic

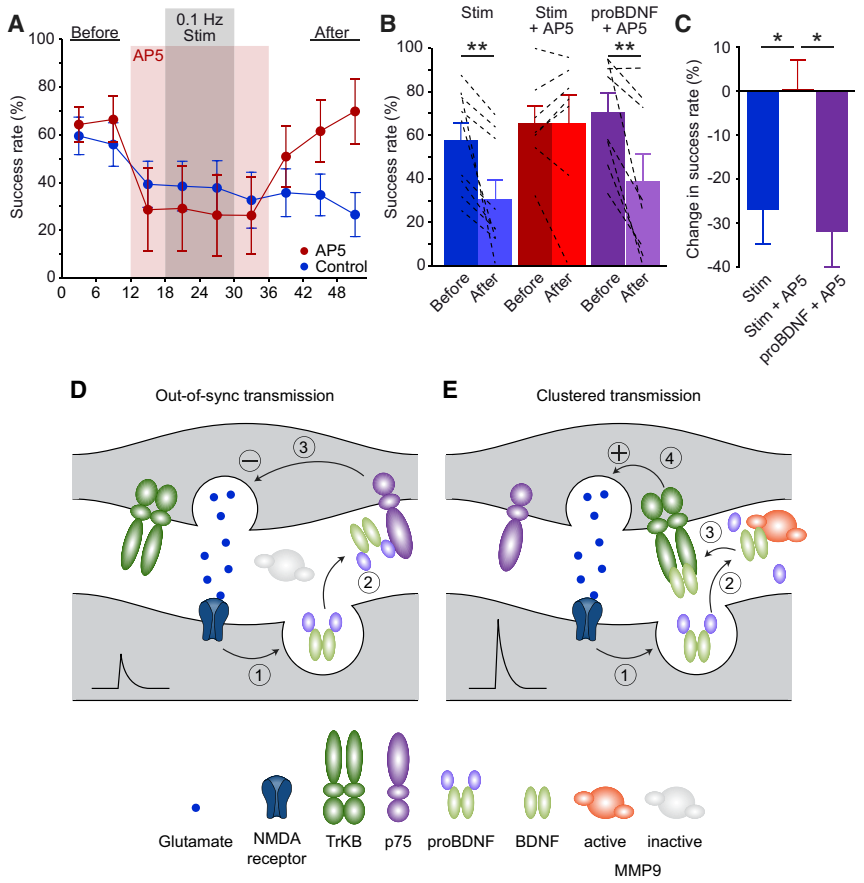

Figure 7. NMDA Receptor Activation Is Required for Depression of Desynchronized Synapses

(A) The success rate of synapses before, during, and after asynchronous stimulation at 0.1 Hz for 12 min. AP5 (50 μM) was applied from the third recording. Calcium transients were either abolished or very low in amplitude during the presence of AP5. The drug was washed out after the first post-stimulation recording. Note that the success rate returned to baseline levels after AP5 wash out, although control synapses remained depressed.

(B) Synaptic success rates before and after asynchronous stimulation (Stim), asynchronous stimulation in the presence of the NMDA receptor antagonist AP5 (Stim + AP5), and after bath application of proBDNF in the presence of AP5 (proBDNF + AP5). AP5 blocks synaptic depression induced by asynchronous stimulation, but not proBDNF-mediated depression (n = 9 [Stim], 7 [Stim + AP5], 8 [proBDNF + AP5] synapses; $^{**}p < 0.01$; paired two-tailed t test).

(C) The changes in success rates differed significantly ($^{*}p < 0.05$; one-way-ANOVA and Fisher's post hoc test). Error bars ± SEM.

(D and E) Putative model of a proBDNF/BDNF-mediated push-pull plasticity mechanism for synaptic clustering.

(D) Glutamate release at desynchronized synapses activates postsynaptic NMDA receptors. NMDA receptor activation triggers release of proBDNF (1). Binding of proBDNF to its high-affinity receptor $p75^{NTR}$ (2) mediates a reduction in presynaptic release probability (3).

(E) NMDA receptor activation at clustered synapses also triggers proBDNF release (1), but MMP9, which is activated or extracellularly released through, for example, increased local dendritic depolarization at clustered synapses, converts proBDNF to BDNF (2). BDNF binds to its receptor TrkB (3) that, in turn, increases presynaptic release probability (4).

clustering and the stabilization of locally synchronized synapses, we conclude that endogenous BDNF is present at clustered synapses and stabilizes synapses at sites of high local co-activity by activating TrkB.

Specifically, we propose the following model of a push-pull plasticity mechanism for synaptic clustering that integrates the data of the present study on BDNF, TrkB, MMP9, and the NMDA receptor with our previous findings on proBDNF/p75 signaling (Winnubst et al., 2015; Figures 7D and 7E). At out-of-sync synapses, glutamate activates postsynaptic NMDA receptors, which in turn mediate the release of proBDNF. proBDNF/BDNF knockdown eliminates clustering cell autonomously, suggesting that proBDNF is released postsynaptically; however, presynaptic release of proBDNF or BDNF may have a role in clustering as well. Binding of proBDNF to $p75^{NTR}$ leads to a reduction in synaptic transmission, probably by reducing synaptic release probability. In contrast, at synapses that are co-active with their neighbors, MMP9 may be activated or released, for example, through enhanced postsynaptic depolarization. Consequently, MMP9 converts proBDNF released after NMDA receptor activation to mature BDNF, which binds to TrkB. TrkB activation increases or stabilizes synaptic transmission.

This model is reminiscent of recently proposed pathways for proBDNF/BDNF-mediated synaptic plasticity in the rodent hippocampus, entorhinal cortex, and neuromuscular junction as well as the *Xenopus* neuromuscular synapse. In particular, there is strong evidence for activity- and NMDA-receptor-dependent release of proBDNF from dendrites of developing hippocampal neurons already at low stimulation frequencies (Nagappan et al., 2009; Orefice et al., 2016; Yang et al., 2009b). Furthermore, proteinases like tissue plasminogen activator or matrix metallopeptidases can convert proBDNF to BDNF upon high-frequency synaptic stimulation (Je et al., 2012, 2013; Nagappan et al., 2009; Yang et al., 2009a). Finally, proBDNF and BDNF modulate presynaptic function in an antagonistic fashion: proBDNF reduces (Gibon et al., 2016; Yang et al., 2009a) and BDNF enhances presynaptic release (reviewed in Park and Poo, 2013).

Whether proBDNF can be released to the extracellular space, where it may act on its receptor or will be cleaved to generate mature BDNF, is a current topic of discussion. Although evidence from mature systems suggest predominant or exclusive

release of BDNF and conversion of proBDNF to BDNF before release (Matsumoto et al., 2008), there is strong evidence for activity-dependent release of proBDNF in the developing hippocampus and the *Xenopus* neuromuscular synapse, as described above (Nagappan et al., 2009; Orefice et al., 2016; Yang et al., 2009b). Together, the data support both the release of proBDNF at immature synapses and its modulatory role on synaptic function through $p75^{NTR}$. The signaling cascades that lead to the activity-dependent release or activation of MMP9 and the conversion of proBDNF to BDNF are currently unknown. Nevertheless, our findings indicate that MMP9 is specifically active at clustered synapses in agreement with previous studies that demonstrated a local function of this metalloproteinase (Dziembowska and Wlodarczyk, 2012).

How BDNF increases presynaptic release has been well characterized. For persistent increases of release, mitogen-activated protein kinase (MAPK) activation through TrkB is required (Cheng et al., 2017; Jovanovic et al., 2000). MAPK, in turn, phosphorylates synaptic-vesicle-organizing proteins of the synapsin family and regulates their interactions with the actin cytoskeleton, potentially enhancing mobilization of synaptic vesicles from the reserve pool (Cheng et al., 2017; Jovanovic et al., 2000). In addition, transient receptor potential-canonical (TRPC) channel activation and calcium release from internal stores can mediate BDNF/TrkB-induced increases in release probability (Amaral and Pozzo-Miller, 2012; Cheng et al., 2017). Whether proBDNF-$p75^{NTR}$ signaling regulates these pathways in an antagonistic manner or whether it recruits different pathways (Oh et al., 2015) will have to be clarified by future studies.

The here-described proBDNF/BDNF-mediated push-pull plasticity acting on individual synapses provides a very efficient and robust plasticity mechanism to generate synaptic clustering. Through antagonistic modulation—depending on the clustering state of a synapse—synaptic function can be fine-tuned within minutes to establish and maintain synaptic clusters. This mechanism should also guarantee that synaptic clusters are spatially restricted, because it allows—in principle—to set a threshold for synaptic potentiation or depression at a given cluster and to prevent synapses of lower local co-activities to be maintained at the edge of a cluster. Together, our results provide insights into how spontaneous activity is able to fine-tune emerging connectivity patterns with single-synapse precision by either depressing out-of-sync synapses through proBDNF/$p75^{NTR}$ signaling when they are asynchronous or stabilizing and potentiating synapses at clustered inputs where proBDNF is converted to BDNF through locally activated MMP9 and subsequent facilitation of presynaptic transmitter release.

EXPERIMENTAL PROCEDURES

Organotypic Slice Preparation

All experimental procedures were approved by the Institutional Animal Care and Use Committee of the Royal Netherlands Academy of Arts and Sciences (licenses Netherlands Institute for Neuroscience [NIN] 10.06 and 11.78). Newborn male or female C57BL/6J mice (P1–P4) were rapidly decapitated, and the dorsal part of the skull together with the overlying skin was removed in order to expose the brain. A horizontal cut was performed in the rostral direction from the border line between the superior and inferior colliculi. The brain region obtained following the cut contained the two hippocampi and was immersed in cold Gey's balanced salt solution (GBSS) for dissection. The two hippocampi were dissected out and positioned on the cutting plate of a tissue chopper (McIlwain), perpendicularly to the blade; 400-μm slices were cut and placed back in cold GBSS solution. Slices were separated from each other and incubated in the same solution at 4°C for 1 hr. Subsequently, each slice was evaluated for the integrity of all hippocampal regions and the entorhinal cortex was removed. Two to four slices were mounted on the membrane of culture inserts (Millipore) already in contact with culture medium (preincubated for 30 min at 37°C and 5% CO_2). Slices were kept in the incubator at 37°C and 5% CO_2 for 2–7 days (Stoppini et al., 1991).

Dye Electroporation

Experiments were performed on visually identified CA3 pyramidal neurons. The recording chamber was perfused with modified Hank's balanced salt solution (HBSS) (Life Technologies) composed of 3.26 mM CaCl2, 0.493 mM MgCl2, 0.406 mM MgSO4, 5.33 mM KCl, 0.441 mM KH2PO4, 4.17 mM NaHCO3, 138 mM NaCl, 0.336 mM Na2HPO4, and 5.56 mM D-glucose, and the temperature was set at 35°C. Individual neurons were then loaded with the calcium indicator dye Oregon Green 488 BAPTA-1 hexapotassium salt (OGB-1) (Life Technologies) by single-cell electroporation (250 μM; 20 ms pulse; ~10 V) with a glass electrode (5 or 6 MΩ). Neurons were left to recover for at least 15 min before imaging. Only cells displaying high synaptic activity and no signs of damage were further considered for imaging.

shRNA-Mediated BDNF Knockdown

The coding sequence for anti-proBDNF/BDNF shRNA (psi-nH1 vector; GeneCopoeia, Rockville, MD) was designed to target a 21-base-pair fragment (5′-GGCGATTCATAAGGATAGACA-3′) found in the transcript variant 10 of mouse and human BDNF mRNA. Hippocampal slices prepared from P1–P3 mice were incubated for 1 or 2 days before transfection. A DNA mix for shRNA (anti-proBDNF/BDNF or scrambled; 1 μg/μL), and either GCaMP6s (0.9 μg/μL) or mCherry (1 μg/μL) was injected through a low-resistance microelectrode at half-depth into the slice right under the CA3 cell layer. The positive pole of tweezer-like electrodes was placed above the slice, and 3 pulses of 1 ms (100-ms interval) were delivered at 27 V (BTX ECM830; Harvard Apparatus, Holliston, MA). The electroporated slices were placed back in the incubator and kept for 4 or 5 days. Synaptic activity was measured at 8 days after birth (total age, postnatal and *in vitro*). Recordings were performed only in slices containing a maximum of 4 labeled pyramidal neurons and in areas without any visually identified axonal labeling. mCherry-expressing neurons were loaded with OGB-1 by dye electroporation. We observed no differences in cellular health, synaptic activity, or clustering between neurons with GCaMP6s or OGB-1.

Calcium Imaging

Images were acquired using a charge coupled device (CCD) camera (iXon+; Andor Technology) mounted on a BX51WI microscope with a 40×/0.8 cone dipping water immersion objective (Olympus). A LED system was used as excitation light source (pE-2; CoolLed). Excitation light was set at 508 nm, and the field of view and excitation restricted to the dendritic region of the cell that was imaged. Frames were acquired at a rate of 30 Hz from three z-planes by means of a piezo-stepper (P-721.LLQ; Physik Instrumente) mounted between microscope and objective, thus resulting in a temporal resolution of at least 10 Hz.

Electrophysiology

Visually identified CA3 pyramidal neurons were maintained at 35°C in a modified HBSS solution (see Dye Electroporation). Electrodes (4 or 5 MΩ; GB150F-8P; Science Products, Hofheim, Germany) were loaded with internal solution (122 mM K-gluconate, 13 mM KCl, 10 mM phosphocreatine di(tris), 10 mM HEPES, 4 mM MgATP, and 0.3 mM Na_3GTP [pH 7.3] with KOH) containing OGB-1 (125 μM). After obtaining the whole-cell configuration, cells were clamped at −70 mV for 15–20 min (MultiClamp 700B; Digidata 1440A; Axon Instruments, Foster City, CA) to allow dye diffusion into the cell. Calcium imaging (as described above) and electrophysiology recordings were acquired

simultaneously. Currents were recorded in voltage clamp (−70 mV), at 10 kHz. Recordings were considered only if the access resistance remained below 30 MΩ. No correction was made for the liquid junction potential.

Stimulation Experiments

In order to trigger activity at single synapses, a glass electrode (5 or 6 MΩ) was inserted in the stratum radiatum of the CA3 region. While imaging the apical dendrites of OBG-1-electroporated cells, a stimulation protocol (5–7 μA; 0.5 ms) was delivered until calcium transients were concomitantly detected on the dendrite. Repeated recordings were made until the success rate of synaptic transmission stabilized. At the end of each experiment, test stimulations were done in the presence of NBQX (10 μM) to verify that the triggered calcium transients were due to monosynaptic transmission.

Image Analysis

Recordings were corrected for drift artifacts by aligning frames using the enhanced correlation coefficient (ECC) algorithm (Evangelidis and Psarakis, 2008). In a set of recordings, each recording was aligned to the first in the series to correct for drift in between recordings. Baseline fluorescence (F_0) was obtained by applying a moving average filter to the aligned stack (window or span = 20 s). A $\Delta F/F_0$ stack was then generated by subtracting and dividing each frame with its counterpart of the F_0 stack. Semi-automated image analysis was performed using custom-made MATLAB software (MathWorks) and ImageJ (NIH). Calcium transients were automatically detected, manually validated, and assigned to synaptic sites as described previously (Winnubst et al., 2015). To determine a threshold for considering a synapse as being activated by BDNF, we carefully analyzed the distribution of activity changes across all synapses after BDNF and BSA control applications (Figure S7). Because we expected increases in synaptic activity after BDNF application, we compared the distributions in the positive range and observed that they differed mostly at activity increases of 1.5/100 s and more (Figure S7A). In fact, the largest difference occurred at the 1.5–2.5/100 s bin (Figure S7B). In addition, we argued that the distribution of activity changes that would occur by chance should distribute symmetrically around zero. Therefore, we subtracted the flipped negative range of the BDNF activity change from the positive distribution and found—again—a maximal difference in the 1.5–2.5/100 s activity increase range (Figure S7C). Together, these observations suggested that synapses that showed activity increases of 1.5/100 s or more had undergone relevant potentiation. Synapses were defined as clustered when their local co-activity was at least 50% higher than co-activity with distant synapses.

Statistics

Data are shown as means ± SEM. To test for clustering, mean co-activity levels were compared between the first and the second distance bins (0–15 μm and 15–30 μm inter-synapse distances, respectively) using an unpaired t test (some synapses lacked neighbors in one of the distance bins). To test for differences in clustering between treatments, co-activity levels in the first distance bin were compared using an independent t test as described previously (Winnubst et al., 2015). One-way ANOVA and Fisher's post hoc test were used for multiple comparisons. The number of occurrences was compared using a chi-square test. The type of test, the number of observations, and the significance levels are specified in the text and/or figure legends.

SUPPLEMENTAL INFORMATION

Supplemental Information includes seven figures and can be found with this article online at https://doi.org/10.1016/j.celrep.2018.07.073.

ACKNOWLEDGMENTS

We thank Helmut Kessels, Christiaan Levelt, Volkmar Lessmann, and Catia Silva for critically reading this manuscript and Johan Winnubst for providing MATLAB scripts for image analysis. This work was supported by grants of the Netherlands Organization for Scientific Research (NWO, Aard- en Levenswetenschappen [ALW] Open Program grants; no. 819.02.017, 822.02.006, and ALWOP.216; ALW Vici, no. 865.12.001, all C.L.; Vidi grant 016.126.361, C.J.W.), a Research Fellowship of the German Research Foundation (DFG) (MI 1448/1-1, K.M.-P.), and a Foundation for Fundamental Research on Matter (FOM) grant (15PR3178, R.v.D.).

AUTHOR CONTRIBUTIONS

D.N., K.M.-P., C.J.W., and C.L. designed experiments. D.N. performed experiments; K.M.-P. and Ü.G. contributed to the local BDNF application experiments. R.v.D. performed the expression analysis. D.N., K.M.-P., and Ü.G. analyzed the data. D.N., K.M.-P., Ü.G., C.J.W., and C.L. interpreted the results. D.N. and C.L. wrote the manuscript.

DECLARATION OF INTERESTS

The authors declare no competing interests.

Received: October 12, 2017
Revised: June 12, 2018
Accepted: July 23, 2018
Published: August 21, 2018

REFERENCES

Amaral, M.D., and Pozzo-Miller, L. (2007). TRPC3 channels are necessary for brain-derived neurotrophic factor to activate a nonselective cationic current and to induce dendritic spine formation. J. Neurosci. *27*, 5179–5189.

Amaral, M.D., and Pozzo-Miller, L. (2012). Intracellular Ca2+ stores and Ca2+ influx are both required for BDNF to rapidly increase quantal vesicular transmitter release. Neural Plast. *2012*, 203536.

Andreska, T., Aufmkolk, S., Sauer, M., and Blum, R. (2014). High abundance of BDNF within glutamatergic presynapses of cultured hippocampal neurons. Front. Cell. Neurosci. *8*, 107.

Aujla, P.K., and Huntley, G.W. (2014). Early postnatal expression and localization of matrix metalloproteinases-2 and -9 during establishment of rat hippocampal synaptic circuitry. J. Comp. Neurol. *522*, 1249–1263.

Berninger, B., and Poo, Mm. (1996). Fast actions of neurotrophic factors. Curr. Opin. Neurobiol. *6*, 324–330.

Brigadski, T., Hartmann, M., and Lessmann, V. (2005). Differential vesicular targeting and time course of synaptic secretion of the mammalian neurotrophins. J. Neurosci. *25*, 7601–7614.

Cabelli, R.J., Hohn, A., and Shatz, C.J. (1995). Inhibition of ocular dominance column formation by infusion of NT-4/5 or BDNF. Science *267*, 1662–1666.

Cabelli, R.J., Shelton, D.L., Segal, R.A., and Shatz, C.J. (1997). Blockade of endogenous ligands of trkB inhibits formation of ocular dominance columns. Neuron *19*, 63–76.

Cabezas, C., and Buño, W. (2011). BDNF is required for the induction of a presynaptic component of the functional conversion of silent synapses. Hippocampus *21*, 374–385.

Cheng, Q., Song, S.-H., and Augustine, G.J. (2017). Calcium-dependent and synapsin-dependent pathways for the presynaptic actions of BDNF. Front. Cell. Neurosci. *11*, 75.

Choo, M., Miyazaki, T., Yamazaki, M., Kawamura, M., Nakazawa, T., Zhang, J., Tanimura, A., Uesaka, N., Watanabe, M., Sakimura, K., and Kano, M. (2017). Retrograde BDNF to TrkB signaling promotes synapse elimination in the developing cerebellum. Nat. Commun. *8*, 195.

Dieni, S., Matsumoto, T., Dekkers, M., Rauskolb, S., Ionescu, M.S., Deogracias, R., Gundelfinger, E.D., Kojima, M., Nestel, S., Frotscher, M., and Barde, Y.A. (2012). BDNF and its pro-peptide are stored in presynaptic dense core vesicles in brain neurons. J. Cell Biol. *196*, 775–788.

Drake, C.T., Milner, T.A., and Patterson, S.L. (1999). Ultrastructural localization of full-length trkB immunoreactivity in rat hippocampus suggests multiple roles in modulating activity-dependent synaptic plasticity. J. Neurosci. *19*, 8009–8026.

Dziembowska, M., and Wlodarczyk, J. (2012). MMP9: a novel function in synaptic plasticity. Int. J. Biochem. Cell Biol. *44*, 709–713.

Edelmann, E., Cepeda-Prado, E., Franck, M., Lichtenecker, P., Brigadski, T., and Leßmann, V. (2015). Theta burst firing recruits BDNF release and signaling in postsynaptic CA1 neurons in spike-timing-dependent LTP. Neuron *86*, 1041–1054.

Ethell, I.M., and Ethell, D.W. (2007). Matrix metalloproteinases in brain development and remodeling: synaptic functions and targets. J. Neurosci. Res. *85*, 2813–2823.

Evangelidis, G.D., and Psarakis, E.Z. (2008). Parametric image alignment using enhanced correlation coefficient maximization. IEEE Trans. Pattern Anal. Mach. Intell. *30*, 1858–1865.

Gibon, J., Barker, P.A., and Séguéla, P. (2016). Opposing presynaptic roles of BDNF and ProBDNF in the regulation of persistent activity in the entorhinal cortex. Mol. Brain *9*, 23.

Hartmann, M., Heumann, R., and Lessmann, V. (2001). Synaptic secretion of BDNF after high-frequency stimulation of glutamatergic synapses. EMBO J. *20*, 5887–5897.

Harward, S.C., Hedrick, N.G., Hall, C.E., Parra-Bueno, P., Milner, T.A., Pan, E., Laviv, T., Hempstead, B.L., Yasuda, R., and McNamara, J.O. (2016). Autocrine BDNF-TrkB signalling within a single dendritic spine. Nature *538*, 99–103.

Huang, Z.J., Kirkwood, A., Pizzorusso, T., Porciatti, V., Morales, B., Bear, M.F., Maffei, L., and Tonegawa, S. (1999). BDNF regulates the maturation of inhibition and the critical period of plasticity in mouse visual cortex. Cell *98*, 739–755.

Iacaruso, M.F., Gasler, I.T., and Hofer, S.B. (2017). Synaptic organization of visual space in primary visual cortex. Nature *547*, 449–452.

Je, H.S., Yang, F., Ji, Y., Nagappan, G., Hempstead, B.L., and Lu, B. (2012). Role of pro-brain-derived neurotrophic factor (proBDNF) to mature BDNF conversion in activity-dependent competition at developing neuromuscular synapses. Proc. Natl. Acad. Sci. USA *109*, 15924–15929.

Je, H.S., Yang, F., Ji, Y., Potluri, S., Fu, X.-Q., Luo, Z.-G., Nagappan, G., Chan, J.P., Hempstead, B., Son, Y.-J., and Lu, B. (2013). ProBDNF and mature BDNF as punishment and reward signals for synapse elimination at mouse neuromuscular junctions. J. Neurosci. *33*, 9957–9962.

Jovanovic, J.N., Czernik, A.J., Fienberg, A.A., Greengard, P., and Sihra, T.S. (2000). Synapsins as mediators of BDNF-enhanced neurotransmitter release. Nat. Neurosci. *3*, 323–329.

Kaplan, D.R., and Miller, F.D. (2000). Neurotrophin signal transduction in the nervous system. Curr. Opin. Neurobiol. *10*, 381–391.

Kerr, A.M., and Capogna, M. (2007). Unitary IPSPs enhance hilar mossy cell gain in the rat hippocampus. J. Physiol. *578*, 451–470.

Kirkby, L.A., Sack, G.S., Firl, A., and Feller, M.B. (2013). A role for correlated spontaneous activity in the assembly of neural circuits. Neuron *80*, 1129–1144.

Kleindienst, T., Winnubst, J., Roth-Alpermann, C., Bonhoeffer, T., and Lohmann, C. (2011). Activity-dependent clustering of functional synaptic inputs on developing hippocampal dendrites. Neuron *72*, 1012–1024.

Lai, K.O., Wong, A.S., Cheung, M.C., Xu, P., Liang, Z., Lok, K.C., Xie, H., Palko, M.E., Yung, W.H., Tessarollo, L., et al. (2012). TrkB phosphorylation by Cdk5 is required for activity-dependent structural plasticity and spatial memory. Nat. Neurosci. *15*, 1506–1515.

Lang, S.B., Stein, V., Bonhoeffer, T., and Lohmann, C. (2007). Endogenous brain-derived neurotrophic factor triggers fast calcium transients at synapses in developing dendrites. J. Neurosci. *27*, 1097–1105.

Larkum, M.E., and Nevian, T. (2008). Synaptic clustering by dendritic signalling mechanisms. Curr. Opin. Neurobiol. *18*, 321–331.

Lavzin, M., Rapoport, S., Polsky, A., Garion, L., and Schiller, J. (2012). Nonlinear dendritic processing determines angular tuning of barrel cortex neurons in vivo. Nature *490*, 397–401.

Lessmann, V., and Brigadski, T. (2009). Mechanisms, locations, and kinetics of synaptic BDNF secretion: an update. Neurosci. Res. *65*, 11–22.

Matsumoto, T., Rauskolb, S., Polack, M., Klose, J., Kolbeck, R., Korte, M., and Barde, Y.-A. (2008). Biosynthesis and processing of endogenous BDNF: CNS neurons store and secrete BDNF, not pro-BDNF. Nat. Neurosci. *11*, 131–133.

McAllister, A.K., Katz, L.C., and Lo, D.C. (1996). Neurotrophin regulation of cortical dendritic growth requires activity. Neuron *17*, 1057–1064.

McGuinness, L., Taylor, C., Taylor, R.D., Yau, C., Langenhan, T., Hart, M.L., Christian, H., Tynan, P.W., Donnelly, P., and Emptage, N.J. (2010). Presynaptic NMDARs in the hippocampus facilitate transmitter release at theta frequency. Neuron *68*, 1109–1127.

Mohajerani, M.H., Sivakumaran, S., Zacchi, P., Aguilera, P., and Cherubini, E. (2007). Correlated network activity enhances synaptic efficacy via BDNF and the ERK pathway at immature CA3 CA1 connections in the hippocampus. Proc. Natl. Acad. Sci. USA *104*, 13176–13181.

Murase, S., and McKay, R.D. (2012). Matrix metalloproteinase-9 regulates survival of neurons in newborn hippocampus. J. Biol. Chem. *287*, 12184–12194.

Nagappan, G., Zaitsev, E., Senatorov, V.V., Jr., Yang, J., Hempstead, B.L., and Lu, B. (2009). Control of extracellular cleavage of ProBDNF by high frequency neuronal activity. Proc. Natl. Acad. Sci. USA *106*, 1267–1272.

Oh, W.C., Parajuli, L.K., and Zito, K. (2015). Heterosynaptic structural plasticity on local dendritic segments of hippocampal CA1 neurons. Cell Rep. *10*, 162–169.

Orefice, L.L., Shih, C.-C., Xu, H., Waterhouse, E.G., and Xu, B. (2016). Control of spine maturation and pruning through proBDNF synthesized and released in dendrites. Mol. Cell. Neurosci. *71*, 66–79.

Palmer, L.M., Shai, A.S., Reeve, J.E., Anderson, H.L., Paulsen, O., and Larkum, M.E. (2014). NMDA spikes enhance action potential generation during sensory input. Nat. Neurosci. *17*, 383–390.

Park, H., and Poo, M.M. (2013). Neurotrophin regulation of neural circuit development and function. Nat. Rev. Neurosci. *14*, 7–23.

Poirazi, P., and Mel, B.W. (2001). Impact of active dendrites and structural plasticity on the memory capacity of neural tissue. Neuron *29*, 779–796.

Richards, G., Messer, J., Malherbe, P., Pink, R., Brockhaus, M., Stadler, H., Wichmann, J., Schaffhauser, H., and Mutel, V. (2005). Distribution and abundance of metabotropic glutamate receptor subtype 2 in rat brain revealed by [3H]LY354740 binding in vitro and quantitative radioautography: correlation with the sites of synthesis, expression, and agonist stimulation of [35S] GTPgammas binding. J. Comp. Neurol. *487*, 15–27.

Sanes, J.R., and Yamagata, M. (2009). Many paths to synaptic specificity. Annu. Rev. Cell Dev. Biol. *25*, 161–195.

Sasi, M., Vignoli, B., Canossa, M., and Blum, R. (2017). Neurobiology of local and intercellular BDNF signaling. Pflugers Arch. *469*, 593–610.

Schinder, A.F., and Poo, M. (2000). The neurotrophin hypothesis for synaptic plasticity. Trends Neurosci. *23*, 639–645.

Smith, S.L., Smith, I.T., Branco, T., and Häusser, M. (2013). Dendritic spikes enhance stimulus selectivity in cortical neurons in vivo. Nature *503*, 115–120.

Stoppini, L., Buchs, P.-A., and Muller, D. (1991). A simple method for organotypic cultures of nervous tissue. J. Neurosci. Methods *37*, 173–182.

Takahashi, N., Kitamura, K., Matsuo, N., Mayford, M., Kano, M., Matsuki, N., and Ikegaya, Y. (2012). Locally synchronized synaptic inputs. Science *335*, 353–356.

Tanaka, J., Horiike, Y., Matsuzaki, M., Miyazaki, T., Ellis-Davies, G.C., and Kasai, H. (2008). Protein synthesis and neurotrophin-dependent structural plasticity of single dendritic spines. Science *319*, 1683–1687.

Vicario-Abejón, C., Collin, C., McKay, R.D., and Segal, M. (1998). Neurotrophins induce formation of functional excitatory and inhibitory synapses between cultured hippocampal neurons. J. Neurosci. *18*, 7256–7271.

Vignoli, B., Battistini, G., Melani, R., Blum, R., Santi, S., Berardi, N., and Canossa, M. (2016). Peri-synaptic glia recycles brain-derived neurotrophic factor for LTP stabilization and memory retention. Neuron *92*, 873–887.

Winnubst, J., Cheyne, J.E., Niculescu, D., and Lohmann, C. (2015). Spontaneous activity drives local synaptic plasticity in vivo. Neuron *87*, 399–410.

Wu, K., Xu, J.L., Suen, P.C., Levine, E., Huang, Y.Y., Mount, H.T., Lin, S.Y., and Black, I.B. (1996). Functional trkB neurotrophin receptors are intrinsic components of the adult brain postsynaptic density. Brain Res. Mol. Brain Res. *43*, 286–290.

Yang, F., Je, H.-S., Ji, Y., Nagappan, G., Hempstead, B., and Lu, B. (2009a). Pro-BDNF-induced synaptic depression and retraction at developing neuromuscular synapses. J. Cell Biol. *185*, 727–741.

Yang, J., Siao, C.J., Nagappan, G., Marinic, T., Jing, D., McGrath, K., Chen, Z.Y., Mark, W., Tessarollo, L., Lee, F.S., et al. (2009b). Neuronal release of proBDNF. Nat. Neurosci. *12*, 113–115.